# Life after recovery: increased resolution of forest resilience assessment sheds new light on post-drought compensatory growth and recovery dynamics

Thomas S. Ovenden[1,2*], Mike P. Perks[2], Toni-Kim Clarke[2], Maurizio Mencuccini[3,4], Alistair S. Jump[1]

[1]Biological and Environmental Sciences, University of Stirling, FK9 4LA, Scotland, UK

[2]Forest Research, Northern Research Station, Roslin, Midlothian EH25 9SY, Scotland, UK

[3]CREAF, E08193 Bellaterra, Barcelona, Spain

[4]ICREA, Pg. Lluís Companys 23, 08010 Barcelona (Spain)

[*] Corresponding author:

Thomas Ovenden

Email: thomas.ovenden@stir.ac.uk

Biological and Environmental Sciences, University of Stirling, FK9 4LA, Scotland, UK

This is the peer reviewed version of the following article: Ovenden, TS, Perks, MP, Clarke, T-K, Mencuccini, M, Jump, AS. Life after recovery: Increased resolution of forest resilience assessment sheds new light on post-drought compensatory growth and recovery dynamics. *Journal of Ecology* 2021; 109: 3157-3170, which has been published in final form at https://doi.org/10.1111/1365-2745.13576. This article may be used for non-commercial purposes in accordance with Wiley Terms and Conditions for self-archiving.

**Abstract**

**1.** Understanding the impacts of extreme drought on forest productivity requires a comprehensive assessment of tree and forest resilience. However, current approaches to quantifying resilience limit our understanding of forest response dynamics, recovery trajectories and drought legacies by constraining the temporal scale and resolution of assessment.

**2.** We compared individual tree growth histories with growth forecasted using dynamic regression at an annual resolution, allowing drought impact and individual tree and stand level recovery dynamics to be assessed relative to a scenario where no drought occurred. The novel application of this approach allowed us to quantify the cumulative impact of drought legacy on radial growth at multiple stem heights at different stand densities.

**3.** We show that the choice of pre- and post-drought periods over which resilience is assessed can lead to systematic bias in both estimates and interpretations of resilience indices. In contrast, measuring growth resilience annually revealed clear non-linearities in tree and stand recovery trajectories. Furthermore, we demonstrate that the influence of pre-drought attributes such as tree size, growth rates and stand densities on growth resilience were only detectable at certain stages of recovery. Importantly, we show that the legacy of drought on tree growth can become positive for some individuals, extending up to nine years after the event such that post-recovery growth can result in

the reclamation of some lost tree and stand basal area.

**4.** *Synthesis*. We demonstrate the importance of increasing the temporal scale and resolution of forest resilience assessment in order to understand both patterns and drivers of drought recovery. We highlight the shortcomings of collapsing growth response into a single average value and show how drought legacy can persist into a post-recovery phase, even positively impacting the growth of some trees. If unaccounted for, this post-recovery growth phase can lead to an underestimation of resilience and an overestimation of above ground losses in productivity, highlighting the importance of considering longer-term drought legacies and compensatory growth on basal area.

# 1. Introduction

Drought-linked losses in forest productivity are now being documented globally (Allen et al., 2015, 2010; Xu et al., 2019). The impact of extreme drought events and other facets of global change on forest systems has direct implications for forest dynamics and ecosystem continuity (Anderegg et al., 2013; Martínez-Vilalta and Lloret, 2016; McDowell et al., 2020) and influences atmospheric feedbacks through reductions in forest carbon stocks and future sequestration potential (Bennett et al., 2015). With extreme drought events expected to increase in both frequency and severity (Szejner et al., 2020), concerns surrounding forest vulnerability to such events (Allen et al., 2015) has seen the application of resilience concepts in forest science become increasingly popular (Nikinmaa et al., 2020).

Our understanding of both ecosystem resilience to extreme drought and losses of net primary productivity (NPP) as a result of these extreme events is intimately linked to both the temporal and spatial scales of assessment. Assessing the resilience of individual trees annually enables the comparison of recovery trajectories between trees, their differential contribution to the stand level response and an estimation of the *time* taken for each tree (and thus the stand collectively) to reach a reference state. Collectively, a fine temporal and spatial scale of assessment could provide much needed insight into the recovery dynamics of the wider forest system.

Understanding when and how a forest recovers following extreme drought has implications for forest management, modelling forest carbon dynamics and our understanding of the

95 structural and functional processes that confer resilience. Forest managers will increasingly
96 depend on knowledge as to which species mixtures (Thurm et al., 2016; Vitali et al., 2018,
97 2017), stand structures or silvicultural prescriptions (Chmura et al., 2011; Drever et al.,
98 2006; Sohn et al., 2016) are best suited to building resilience and adaptive capacity to deal
99 with the projected increases in frequency and intensity of extreme drought events (Dai,
100 2013).
101
102 Altering tree density or size class distributions is a key mechanism by which the structure of
103 existing forests can be modified to adapt to changing conditions (Jump et al., 2017; Sohn et
104 al., 2016), with the expectation that a lower stand density can increase the water availability
105 for remaining trees and reduce drought stress (Manrique-Alba et al., 2020). Deciding on an
106 optimal stand density, silvicultural prescription or selecting which trees to retain is however
107 complex. A growing body of work is highlighting how the effectiveness of forest
108 management in mitigating the negative effects of drought is contingent on the interplay
109 between the timing and intensity of interventions, stand age, elevation, soil conditions, tree
110 size and species (Gazol et al., 2017; Kerhoulas et al., 2013; Martínez-Vilalta et al., 2012; Seidl
111 et al., 2017; Sohn et al., 2016). As a result, understanding the behaviour of individual trees,
112 their collective contribution to the stand and factors that pre-dispose poor drought
113 performance will be crucial to effectively manage and manipulate stand structure to
114 increase future resilience.
115
116 Many assessments of forest resilience to drought focus on measuring the ability of a forest
117 to return to a previous average growth rate and assume the climate driving growth is
118 unchanged (Gazol et al., 2017; Lloret et al., 2011). This view implicitly assumes that the pre-

119 disturbance state is the desirable state to which a system should return and fails to account
120 for how climatically favourable to growth pre- or post-drought years were. As a result, pre-
121 drought growth may not be the most suitable benchmark against which resilience or
122 recovery is assessed, since we may erroneously infer that recovery has or has not occurred
123 and systematically under- or overestimate the true loss of radial growth.
124
125 To better quantify the total impact of a particular drought event it is preferable to estimate
126 the cumulative loss of growth over time relative to a scenario where that drought was
127 absent. While rarely quantified in studies of forest resilience (*cf.* Thurm et al., 2016), the loss
128 of basal area (BA) as a direct result of drought is of clear relevance to both forest managers
129 and in modelling carbon dynamics, since it is a direct measure of the cumulative impact of
130 lost radial growth and above ground productivity.
131
132 The spatial scale at which resilience is assessed can also influence both our understanding of
133 drought resilience and measures of drought legacy. Hoffmann et al., (2018) showed an
134 increase in resilience with stem height for *Picea abies*, but a decrease or no change with
135 stem height for four other gymnosperms from different genera (*Thuja, Tsuga, Cryptomeria*
136 *and Metasequoia*). Similarly, the magnitude and direction of these changes in resilience
137 with stem height varied between species (Hoffmann et al., 2018). These findings question
138 how representative tree cores collected at breast height (and the indices derived from
139 them) are of whole-tree drought response. Similarly, individual trees can show considerable
140 variability in drought response, with larger trees tending to be more negatively impacted by
141 drought in terms of both growth and mortality (Bennett et al., 2015; Stovall et al., 2019)
142 while faster growing trees sometimes suffer a greater immediate growth impact than their

143 slower growing conspecific neighbours (Martínez-Vilalta et al., 2012). These studies indicate
144 that patterns in growth resilience, drought impact and divergent patters of recovery at the
145 tree level hold key information needed to explain contrasting patterns in drought resilience
146 observed at the stand scale. Similarly, these studies suggest that the pre-drought attributes
147 of individual trees and the stand collectively can be good predictors of drought performance
148 and recovery such that important detail is lost when the temporal resolution of assessment
149 is too coarse or the timescale too short.
150
151 Using *Pinus sylvestris* tree-ring chronologies, we compare methods and test for biases in a
152 common approach to calculating forest resilience to an extreme drought event. Then, using
153 dynamic regression to capture individual tree climate-growth relationships and growth
154 histories, we forecasted annual growth rates at three different stem heights and two stand
155 densities for nine years after this same extreme drought event to simulate a scenario where
156 no drought had occurred. We modified the resilience index proposed by Lloret et al., (2011)
157 to calculate growth resilience annually as well as quantifying growth and size deficits over
158 these nine years to test the following hypotheses:
159
160 1) Given the differences in resilience with stem height documented in other coniferous
161 species (Hoffmann et al., 2018), we hypothesise that resilience will change with stem
162 height in *Pinus sylvestris*.
163
164 2) Patterns in growth resilience over time at the stand level will be due to the
165 disproportionate influence of some trees on stand recovery.

3) Faster growing, larger and more densely spaced trees will show lower growth resilience relative to slower growing, smaller and lower density trees under extreme drought throughout the post-drought period.

# 2. Materials and Methods

### 2.1. Site description and management history

This research was conducted in a monospecific spacing experiment of *Pinus sylvestris* established in 1935 on a relatively sheltered site in the north-east of Scotland (57° 36′ 23″ N, 4° 16′ 50″ W). The site sits at an elevation of 170m a.s.l with an average slope of 5 degrees. A surface water gley is the dominant soil type throughout and mean annual rainfall over the study period (1961 – 2002) is 851mm, with November being the wettest month on average.

Two spacing treatments were used in the present study representing high ($\rho_H$) and low ($\rho_L$) density stands. At the time of sampling (2002-2003), these plots were stocked at 1047 live trees per hectare ($\rho_H$) and 647 live trees per hectare ($\rho_L$). Some pruning was carried out in the 1950's and 1960's but no thinning or other management has been carried out during the life of the stand.

### 2.2. Dendrochronological data

34 trees from each of the two treatments ($\rho_H$ and $\rho_L$) were felled in 2002-2003 and cross-sectional discs were taken along the length of each tree approximately every metre. These discs were digitised and all disc images within ± 30cm from 0.3, 1.3m and 3.3m high were selected from both $\rho_H$ and $\rho_L$ for use in the present study. This approach ensured that

189 measurements were consistently taken from a similar stem height, whilst allowing for some
190 variation in the precise location of each disc (e.g. due to the location of branch whorls). As a
191 result of these criteria, not all trees are represented at all three stem heights.
192
193 Annual ring widths were measured using two separate radii from each scanned disc image
194 using WinDENDRO image analysis software (Regents Instruments, Quebec). Both radii were
195 averaged to give a mean annual radial increment for each disc and each chronology was
196 subsequently crossdated following the leave-one-out principle on overlapping segments
197 using the *dplR* package (Bunn et al., 2019) to ensure each ring was accurately dated. Raw
198 ring width (RW) data were then converted into individual tree annual basal area increments
199 (BAI) (**Fig. S1**) following **Eq. 1,**
200
201 **Eq. 1**
202
203 $$BAI = \pi(R_t^2 - R_{t-1}^2)$$
204
205 where *R* is the radius of the tree in year *t*. BAI was used instead of raw ring widths as it
206 better represents annual tree growth than linear measures such as ring width (Biondi and
207 Queaan, 2008) and was required for calculations of both growth and size deficit. Basal area
208 (BA) was then calculated annually for each tree as the cumulative sum of BAI records up to
209 and including each year as a measure of annual tree size. Crossdating and the conversion of
210 raw ring width data into BAI for each disc was conducted using *dplR* package (Bunn et al.,
211 2019) using R version 3.6.1 (R Core Team, 2019).
212

213

214 **2.3. Extreme drought year identification**

215 We calculated both the Standardized Precipitation Evapotranspiration Index (SPEI) (Vicente-
216 Serrano et al., 2010) for August using a six-month integration window ($SPEI_{Aug6}$) and the
217 Climatic Water Deficit (CWD) over the study period (1961 – 2002) to identify any extreme
218 drought events in the climate record. CWD was calculated monthly using a Thornthwaite-
219 type water-balance model following (Lutz et al., 2010) as the difference between Potential
220 Evapotranspiration (PET) and Actual Evapotranspiration (AET) using code developed by
221 (Redmond, 2019). Interpolated climate data at 1km resolution, obtained from the Climate
222 Hydrology and Ecology Research Support System (CHESS) meteorology dataset for Great
223 Britain (Robinson et al., 2017) for the study period (1961 – 2002) was used for both SPEI and
224 CWD. Both drought indices were used since the reliance on SPEI as the only drought index
225 has been shown to occasionally misclassify drought conditions (Zang et al., 2019). More
226 negative SPEI values indicate progressively more severe drought conditions, with extreme
227 droughts commonly considered to be at an SPEI threshold of < –2 (Hoffmann et al., 2018;
228 Vanhellemont et al., 2018), which was also the threshold adopted here. To identify extreme
229 drought years using CWD values, we summed monthly CWD values over 12 months (Jan –
230 Dec) every year. Only 1984 was classified by SPEI as an extreme drought year while the CWD
231 analysis confirmed this year showed the largest CWD across years in the study period. 1984
232 also corresponds to a period of growth depression in the tree-ring record at all disc heights
233 in both treatments (**Fig. S1**). As such the 1984 drought year was selected for further analysis
234 in the present study.

235

### 2.4. Climate variables

To include climate variables that correlate strongly with radial growth in *P. sylvestris* (Jyske et al., 2014; Misi et al., 2019) as both predictors in dynamic regression models and when forecasting BAI values in a no-drought scenario, we calculated total precipitation and growing degree days above 5°C ($gdd$) annually from 1961- 1993 using 1km resolution interpolated climate data (Met Office et al., 2019). Annual precipitation ($Precip_{sum}$) was calculated by summing daily precipitation across the whole year while $gdd$ was calculated for each year using temperature data from Jan – Sept (273 days) in the *pollen* package in R (Nowosad, 2019) following **Eq. 2**,

**Eq. 2**

$$gdd = \sum_{i=j}^{273} (T_i - 5), \quad if \quad T_i > 5$$

where annual $gdd$ is the sum of the positive differences between daily mean air temperature ($T_i$) with a threshold value of +5°C from Jan – Sept (273 days). We chose *gdd* as it has previously been used to effectively study the onset and duration of tracheid production in *P. sylvestris* (Jyske et al., 2014), with 5°C frequently used as a *gdd* threshold in this species (Jyske et al., 2014; Seo et al., 2008). We included late winter temperatures (Jan-Feb) in the calculation of $gdd$ as it has been found to be positively correlated with ring width in previous studies of *P. sylvestris* in Scotland (Grace and Norton, 1990), though its inclusion had a minimal effect on final $gdd$ values. Equally, we chose to include all of September in calculating $gdd$ to accommodate for the extended growing season and duration of tracheid development at our more southerly study site than documented in *P. sylvestris* at more northern latitudes (Jyske et al., 2014).

### 2.5. Dynamic regression analysis and BAI forecasting

Focusing on the 1984 extreme drought year, we fitted dynamic regression models to each chronology at each stem height in both density treatments from 1961 – 1983 (the year before the 1984 drought) following **Eq. 3**,

**Eq. 3**

$$BAI_t = \beta_0 + \beta_1 Precip_{sum_{1,t}} + \beta_2 gdd_{2,t} + \beta_3 SPEI_{Aug6_{3,t}} + \eta_t$$

where $BAI_t$ is the annual BAI at time *t*, $\beta_0$ is the overall intercept, $Precip_{sum}$, $gdd$ and $SPEI_{Aug6}$ are climate predictors at time *t*, and the errors from the regression, $\eta_t$ are modelled as an autoregressive integrated moving average (ARIMA) *p, d, q* process (where *p, d* and *q* represent the auto-regressive order, the degree of differencing and the moving average order, respectively). The multiple regression part of the model captures each chronology's relationship between growth and climate prior to the 1984 drought event. The ARIMA part of the model accounts for each chronology's unique short-term time series dynamics, with each forecasted value incorporating lagged values of the dependant variable (or its forecasted values) as well as lagged model errors (to the order of *p* and *q* respectively). As such, dynamic regression combines exogenous predictors with the history of the time series in a single model (Hyndman and Athanasopoulos, 2018).

For each chronology at each stem height in both density treatments a large number of possible *p, d, q* values were calculated to identify the best fitting ARIMA model for the

283 regression errors. The number of differences (*d*) to achieve stationarity of the data was
284 calculated using a KPSS test (Hyndman and Athanasopoulos, 2018), while optimal *p* and *q*
285 values were chosen by minimising the AICc values. To ensure the maximum number of
286 possible ARIMA models were fitted and the minimum AICc value was found, both
287 approximation parameters and the use of stepwise procedures were relaxed. For each
288 chronology's best fitting dynamic regression model, we checked that the residuals were
289 normally distributed and that the ARIMA errors were free of autocorrelation by plotting an
290 autocorrelation function (ACF), resulting in the successful fitting of individual dynamic
291 regression models to 120 chronologies.
292
293 For 1984 (the drought year), values for all three climate variables ($Percip_{sum}$, $gdd$ and
294 $SPEI_{Aug6}$) were replaced by their average values for the period between 1961-1983, thus
295 replacing the observed extreme climate values in 1984 with average climate values. The
296 mean 1984 values for these three climate variables and the observed annual values for
297 these same variables from 1985-1993 were then used in conjunction with each chronology's
298 individually fitted dynamic regression model to forecast annual BAI values ($BAI_{for}$) and 95%
299 confidence intervals for each year between 1984 - 1993 in a scenario where no drought had
300 occurred (**Figs. S2–7**). Forecasted BAI values for each tree were then plotted and visually
301 sense checked. We chose to forecast BAI for nine years following the 1984 drought to avoid
302 the influence of any conditions immediately preceding 1995, the next (though less severe)
303 drought identified in the climate record.
304
305 Each chronology's BA in 1983 was calculated by summing all observed annual BAI values up
306 to and including 1983. Forecasted annual BAI values were then added to the same

chronology's BA in 1983 to calculate the forecasted annual basal area ($BA_{for}$) of each chronology at all three stem heights in both treatments. As such $BAI_{for}$ and $BA_{for}$ represent individual tree annual growth and size, respectively in a scenario where the extreme drought of 1984 had never occurred but was instead a climatically average year. All dynamic regression modelling and forecasting was carried out using the *forecast* package in R (Hyndman et al., 2020).

### 2.6. Pre- and post-drought average growth resilience

Resilience (*Rs*) assessment, as proposed by Lloret et al., (2011), compares a pre-drought growth average with a post drought growth average following **Eq. 4**,

**Eq. 4**

$$\text{Resilience } (Rs) = \frac{Post_{Dr}}{Pre_{Dr}}$$

where $Pre_{Dr}$ and $Post_{Dr}$ are the average pre- and post-drought growth rates (respectively), calculated using the same number of pre- or post- drought years. We refer to the size of this period over which growth is averaged as an integration period throughout the remainder of this text. The same number of pre-drought and post-drought years were always used to calculate the respective averages for an integration period. To assess the influence of the size of the chosen integration period on our interpretation of resilience, we calculated resilience for all three stem heights in both density treatments for 2, 3, 4, 5 and 6 year integration periods following **Eq. 4** using the *PointRes* package (van der Maaten-Theunissen

et al., 2015) to reflect a range of integration periods commonly chosen in studies of forest resilience.

To investigate differences in *Rs* between integration periods, we used *lme4* (Bates et al., 2015) to fit a linear mixed effects model following **Eq. 5**,

**Eq.5**

$$Rs_{ij} = X_{ij}\beta + b0_i + b1_i X_{ij} + \varepsilon_{ij}$$

Where $Rs_{ij}$ is the resilience for the *j*th measure of the *i*th tree, $X$ is an *n* x *p* matrix of fixed effect variables, including integration period, stem height and stand density, $\beta$ is a *p* x *1* column vector of regression estimates, $b0_i$ represents the random effect of tree, where $b0_i$ ~ $N(0,\sigma^2_0)$ and the random slope is $b1_i$ ~ $N(0,\sigma^2_1)$. We used log transformed *Rs* values as this improved model fit. The most parsimonious model was selected using *pbkrtest* (Halekoh and Højsgaard, 2014), dropping stand density as a non-significant fixed effect ($p > 0.05$). The final model fit integration period and stem height as fixed effects and tree ID and integration period as random effects. Significance values were obtained from model output using the *lmerTest* package (Kuznetsova et al., 2017).

### 2.7. Growth resilience

We combined the growth rates forecasted using dynamic regression with the observed growth rates at an annual scale to calculate resilience. In doing so we quantified resilience of both individual trees and average stand response for growth resilience (*Gr*) (the ability to return to forecasted growth rates) using **Eq. 6**. For *Gr*, we modified the resilience calculation

352 introduced by Lloret et al., (2011) by replacing the pre-drought growth average with the
353 forecasted growth rate ($BAI_{for}$) in a given year,
354
355 **Eq. 6**

$$\text{Growth resilience } (Gr) = \frac{BAI_{obs}}{BAI_{for}}$$

356
357 where $BAI_{obs}$ is the observed basal area increment in a given year, $BAI_{for}$ is the forecasted
358 basal area increment for that same year. We calculated *Gr* for 1984 and then annually for
359 the following 9 years (1985 – 1993) for each chronology individually and on average at all
360 three stem heights in both treatments.
361
362 We subsequently fit mixed-effect models using *nlme* (Pinheiro et al., 2020) to investigate
363 the change in *Gr* over time and assess the importance of stand density ($\rho_H$ and $\rho_L$), stem
364 height (0.3m, 1.3m or 3.3m) and individual tree pre-drought growth rate ($BAI_{1983}$) and size
365 ($BA_{1983}$) for the year preceding the extreme drought of 1984. We used *nlme* over *lme4* for
366 this analysis as it allowed us to fit a correlation structure. Both pre-drought growth rate and
367 size were standardised to have a mean of zero and a SD of one to ensure estimated
368 coefficients were on the same scale, while *Gr* was log transformed to improve both the
369 normality of the residuals and satisfy model assumptions. To account for the non-linearity in
370 *Gr* over time, we first identified the optimal number of degrees of freedom to fit natural
371 cubic splines to year using AIC values. The optimal autocorrelation structures were also
372 determined using AIC values and log likelihood ratio tests. The correlation structure for *Gr*
373 was modelled using a corARMA correlation structure set to *p=1*, *q=1* and four degrees of

freedom were specified for the natural splines fit to year. Initially, $BAI_{1983}$, $BA_{1983}$, stem height and stand density were fit as fixed effects along with their interaction with year/time. As all interactions were significant ($p < 0.05$), the final model was fit following **Eq. 7**,

**Eq. 7**

$$Gr_{ij} = X_{ij}\beta + b0_i + \varepsilon_{ij}$$

Where $Gr_{ij}$ is the growth resilience for the *j*th measure of the *i*th tree, $X$ is an *n* x *p* matrix of fixed effect variables, including *year* fit using natural cubic splines with four degrees of freedom, *stem height*, *stand density*, $BAI_{1983}$ and $BA_{1983}$, with retained significant interactions ($p < 0.05$) between all fixed effects and *year*, $\beta$ is a *p* x *1* column vector of regression estimates, $b0_i$ represents the random effect of *tree*, where b0i ~ N (0,$\sigma^2_0$) and ε represents error term, where $\varepsilon_i$ ~ N (0, σ2). No residual autocorrelation was detected using ACF plots. Adjusted marginal means and unadjusted 95% confidence intervals were obtained using the R package *emmeans* (Lenth, 2016) and comparisons for retained interactions made using the *'contrast'* function to assess effects at the annual scale. As pre-drought growth and size are continuous variables, the effect of $BAI_{1983}$ and $BA_{1983}$ was compared in *emmeans* annually using quantiles.

### 2.8. Annual size and growth deficit

To fully capture both growth and size recovery trajectories, we calculated the annual (BAI) and cumulative (BA) loss of radial increment for individual trees and summed across all trees at each stem height in both treatments by subtracting forecasted from observed values every year between 1984-1993. The year in which an individual tree achieved the

forecasted annual growth rate (BAI), or size (BA) was considered to represent the year in which a given tree fully recovered to a growth rate or size expected in a scenario where no drought had occurred i.e. complete recovery. We also forecasted annual ring width index values for all trees at 0.3m in both $\rho_H$ and $\rho_L$ using the same ring width data detrended using a cubic smoothing spline with a 30-year cut off. We then used these forecasted values to calculate tree and stand level annual size and growth deficits in the same way as for the BAI data to ensure our results derived from BAI values were robust.

# 3. Results

### 3.1. Growth Resilience

Mixed-model results comparing *Rs* calculated over different integration periods indicates a significant linear increase in *Rs* with the size of the integration period ($p = < 0.001$) (**Fig. 1, Table 1**). Stem height showed a significant ($p = 0.023$) but weak negative relationship with *Rs*, indicating *Rs* decreases with increasing stem height (**Table 1**).

**Table 1 –** Mixed-effects model output for resilience values calculated using different numbers of pre- and post-drought years (integration periods = 2, 3, 4, 5 and 6 years) at three different stem heights (0.3m, 1.3m and 3.3m) for trees in both high ($\rho_H$) and low ($\rho_L$) density stands considered collectively.

| Fixed effect | Estimate | Std. Error | df | t value | p-value |
|---|---|---|---|---|---|
| (Intercept) | **-0.279** | **0.018** | **73.586** | **-15.800** | **<0.001** |

| | | | | | |
|---|---|---|---|---|---|
| Integration period | **0.044** | **0.003** | **61.962** | **14.833** | **<0.001** |
| Stem height | **-0.007** | **0.003** | **514.627** | **-2.287** | **0.023** |

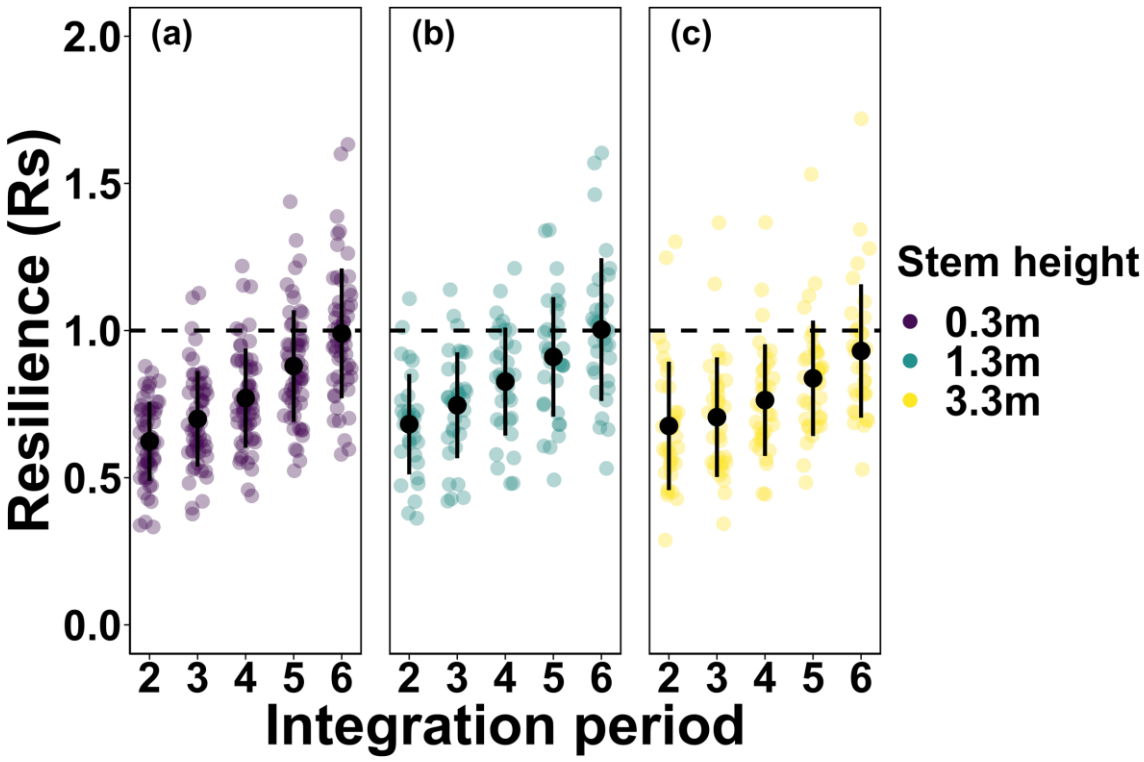


**Figure 1** - Resilience values calculated using different numbers of pre- and post-drought years (integration periods = 2, 3, 4, 5 and 6 years) for three stem heights (a) = 0.3m with *n* = 56, (b) = 1.3m with *n = 33* and (c) = 3.3m with *n = 35*, pooled across both high ($\rho_H$) and low ($\rho_L$) density treatments. The same number of pre- and post-drought years were used to calculate pre- and post-drought growth averages for each integration period. Each coloured dot represents a tree while black dots and lines represent the mean resilience value ±1 SD respectively for each integration period. Individual points are displayed as 'jittered' (small amount out random variation added to the x axis values) to better discern individual data points.

The analysis of growth resilience calculated annually using forecasted values shows a contrasting and more complex pattern in resilience over time than that observed using pre- and post-drought growth averages, with a clear non-linear pattern in *Gr* emerging for all stem heights in both high density ($\rho_H$) and low density ($\rho_L$) treatments (**Fig. 2**). Mixed-model results that account for both this non-linearity and autocorrelation in annual values of *Gr* show significant interactions between year and stem height, stand density, $BAI_{1983}$ and $BA_{1983}$ (**Table 2**).

A comparison of the estimated marginal means for *Gr* at each year for stand density and for different quantiles of $BAI_{1983}$ and $BA_{1983}$ found that differences were only detectable at certain periods during drought recovery (**Fig. S8**). Differences in *Gr* between trees based on pre-drought growth rate ($BAI_{1983}$) were only detected between 1985 and 1987 (the three years following drought), during which trees with higher $BAI_{1983}$ showed significantly higher *Gr* (**Fig. S8a**). Similarly, higher density stands ($\rho_H$) showed greater *Gr* than lower density stands ($\rho_L$), but only between 1985-1986 (**Fig. S8c**), corresponding to the two-year period of continued growth decline post-drought (**Fig. 2–4**). In contrast, smaller trees (lower $BA_{1983}$) showed consistently higher Gr, from 1986 – 1993 (**Fig. S8b**).

At the individual tree level, patterns in *Gr* trajectories show considerable differences in the time taken to recover, with some trees at all stem heights in both density treatments never achieving forecasted levels (**Fig. 3**). Across all stem heights in both density treatments, full recovery occurred anywhere between one- and six-years post drought (**Fig. 3**), however the

majority of those trees that recovered to forecasted growth rates did so between three- and six-years post drought.

**Table 2** – Type 3 ANOVA summary of the mixed-effects model output for growth resilience (*Gr*) calculated annually for all stem heights and both density treatments (*n = 120*) and reported on the *log* transformed scale. Chisq = Wald Chi-square, *df* = degrees of freedom, $BA_{1983}$ = basal area in 1983, $BAI_{1983}$ = basal area increment in 1983 and interaction terms are denoted by ×. Significant values are highlighted in bold ($p < 0.05$).

| **Fixed effect** | **Chisq** | ***df*** | **p-value** |
|---|---|---|---|
| (Intercept) | **22.24** | **1** | **<0.001** |
| Year | **160.63** | **4** | **<0.001** |
| Stem height | 3.00 | 2 | 0.224 |
| Plot | 3.28 | 1 | 0.070 |
| $BA_{1983}$ | 0.24 | 1 | 0.627 |
| $BAI_{1983}$ | 2.78 | 1 | 0.095 |
| Year × Stem height | **17.64** | **8** | **0.024** |
| Year × Stand density | **22.56** | **4** | **<0.000** |
| Year × $BA_{1983}$ | **12.62** | **4** | **0.013** |
| Year × $BAI_{1983}$ | **18.84** | **4** | **<0.001** |

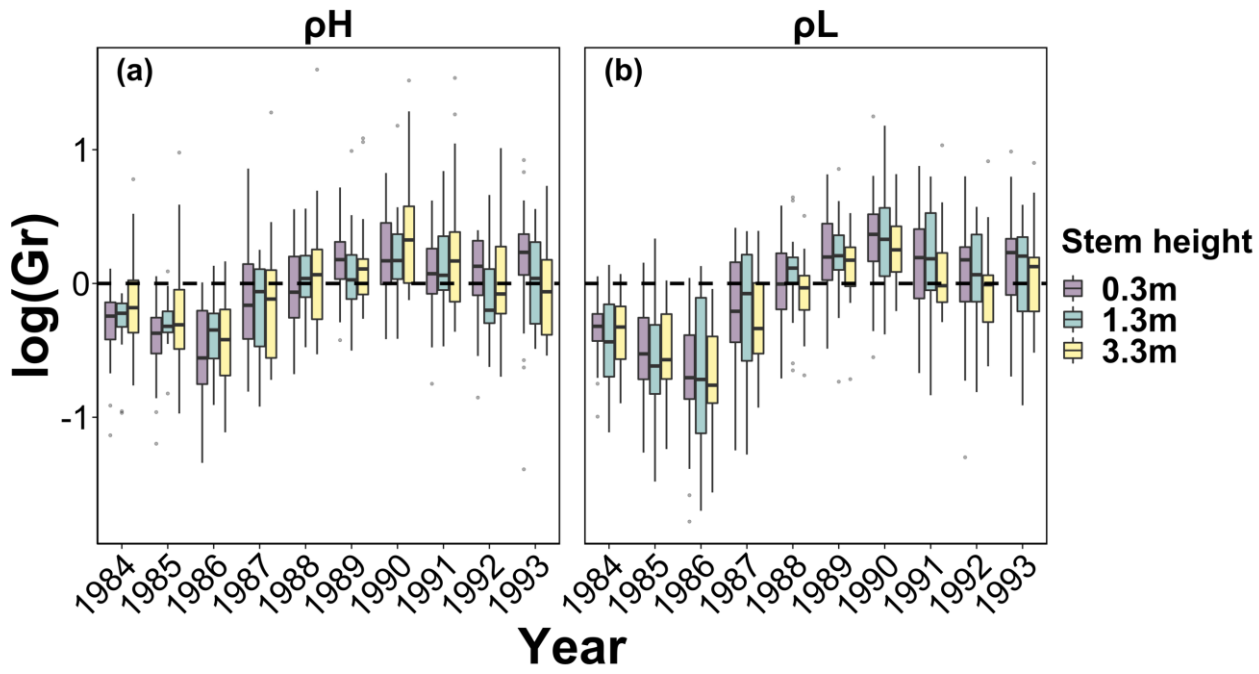


**Figure 2** – Box-plots showing median growth resilience (*Gr*) for (a) high density ($\rho_H$) and (b) low density ($\rho_L$) treatments for all three stem heights considered in this study (0.3m, 1.3m and 3.3m) calculated annually for the drought year (1984) and the subsequent 9 years (1985-1993). The dashed horizontal black line indicates whether growth recovered (above) or not (below), relative to forecasted values. Hinges show first and third quantiles while whiskers show largest and smallest values (excluding outliers) while outliers are indicated by points beyond the whiskers.

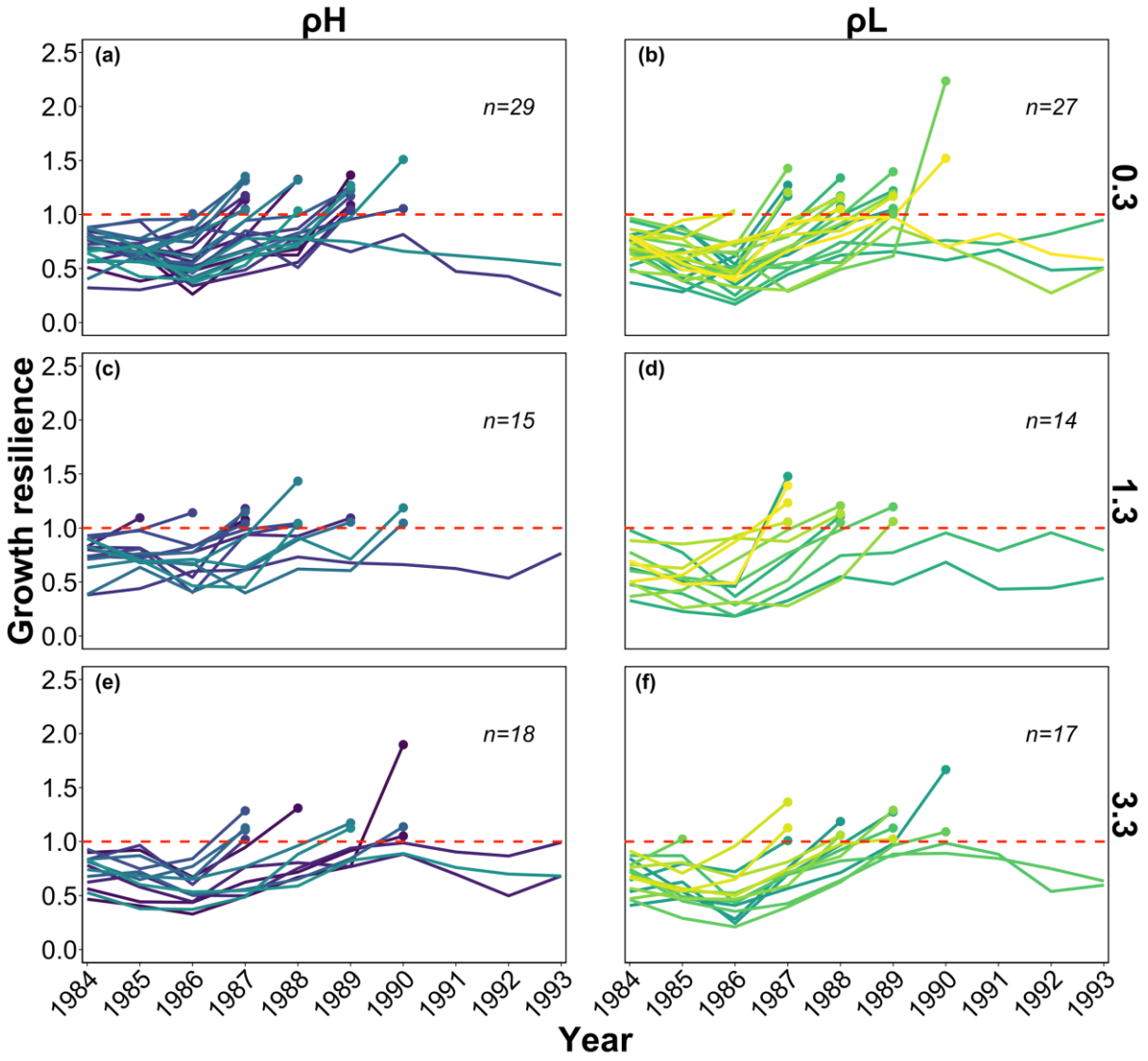


475

476 **Figure 3** – Individual tree annual growth resilience (*Gr*) values for (a, b) 0.3m, (c, d) 1.3m and

477 (e, f) 3.3m stem heights in both high ($\rho_H$) and low ($\rho_L$) stand density treatments. Values >1

478 (above the red dashed line) indicate growth recovery has occurred (observed growth rates

479 achieved forecasted values) while values < 1 (below the red dashed line) indicate a tree is

480 still in growth recovery. Each line respresents a different tree and points at the terminus of

481 the same line correspond to the year in which that same tree reached forecasted growth

482 rates. *Gr* values for years following growth recovery are not displayed.

483

### 3.2. Size and growth deficit

In terms of absolute loss of annual growth, all three stem heights in both density treatments showed a progressive growth decline in the two years following the 1984 drought, with the lowest annual growth record for all three stem heights in both treatments being 1986 with the exception of 1.3m in $\rho_L$ which was marginally lower in 1985 (**Fig. 4, Table S1**).

In 1987, summed annual growth rates for all trees in each treatment and at all three stem heights showed a large reversal of the progressive growth decline of the previous three years (the pattern of continued growth decline reversed and growth recovery began) (**Fig. 4**). Despite a reversal of the continued decline in growth performance, annual stand growth at each stem height and in both treatments continued to underperform relative to forecasted growth. As a result, the cumulative loss of basal area continue to decline into 1987 for 1.3m in both $\rho_H$ and $\rho_L$, and into 1988 for all remaining stem heights in both treatments (**Fig. 4, Table S1**).

By 1989 observed annual stand growth rates in both $\rho_H$ and $\rho_L$ were better than forecasted at all stem heights (**Fig. 4, Table S1**)**.** This return to forecasted growth indicates that complete stand level growth recovery had effectively occurred by 1989, five years after drought. In subsequent years, stand growth rates at all stem heights and in both treatments continued exceeding forecasted growth rates which in turn resulted in a reversal and progressive reclamation of lost BA in the years following 1989 (**Fig. 4**).

While growth recovery at all stem heights in both density treatments occurred at the stand level, full size recovery (that is, observed tree size achieving forecasted tree size in a no

508 drought scenario) never occurred for any stem height in either treatment, despite the
509 growth rate of many trees exceeding forecasted values. For 3.3m and 1.3m heights in both
510 density treatments, observed annual growth for all trees collectively (summed) dropped
511 back to values that were almost indistinguishable from forecasted values in 1992 and 1993,
512 which in turn resulted in size recovery plateauing at below forecasted levels (**Fig. 4**). In
513 contrast, summed annual growth always remained above forecasted values at 0.3m in both
514 density treatments from 1989 onwards. Of particular note is a clear apex in annual growth
515 rate in 1990 for summed annual growth across all trees both collectively (**Fig. 4**) and on
516 average (**Fig. 2**) relative to forecasted growth rates.
517
518 The observed patterns of summed annual growth and partial size recovery is the result of a
519 stratification of individual growth performances in the years following drought and the
520 disproportionate contribution to summed growth of overperforming individuals (**Fig. 4**).
521 Conversely, some trees never fully recovered to forecasted growth rates (**Fig. 3**) or
522 sufficiently overcompensated their growth to recover lost BA (**Fig. 4**). On average, all three
523 stem heights in both $\rho_L$ and $\rho_H$ no longer showed a negative growth resilience by 1989 (**Fig.**
524 **2**), indicating that by 1989, median tree size was no longer different from a scenario where
525 the 1984 drought had never occurred.
526
527 The general pattern of a progressively severe growth depression (and thus decreasing
528 resilience) in the years following the 1984 drought (**Figs 2**–**3**), followed by an
529 overcompensation of growth (**Fig. 4**), is also clear from the mean BAI values for each stem
530 height in both treatments (**Fig. S1**). The observed patterns and timing of both growth and
531 size recovery trajectories were also observed using ring width data detrended using cubic

smoothing spline with a 30-year cut off for all trees at 0.3m in both density treatments (**Fig. S9**).

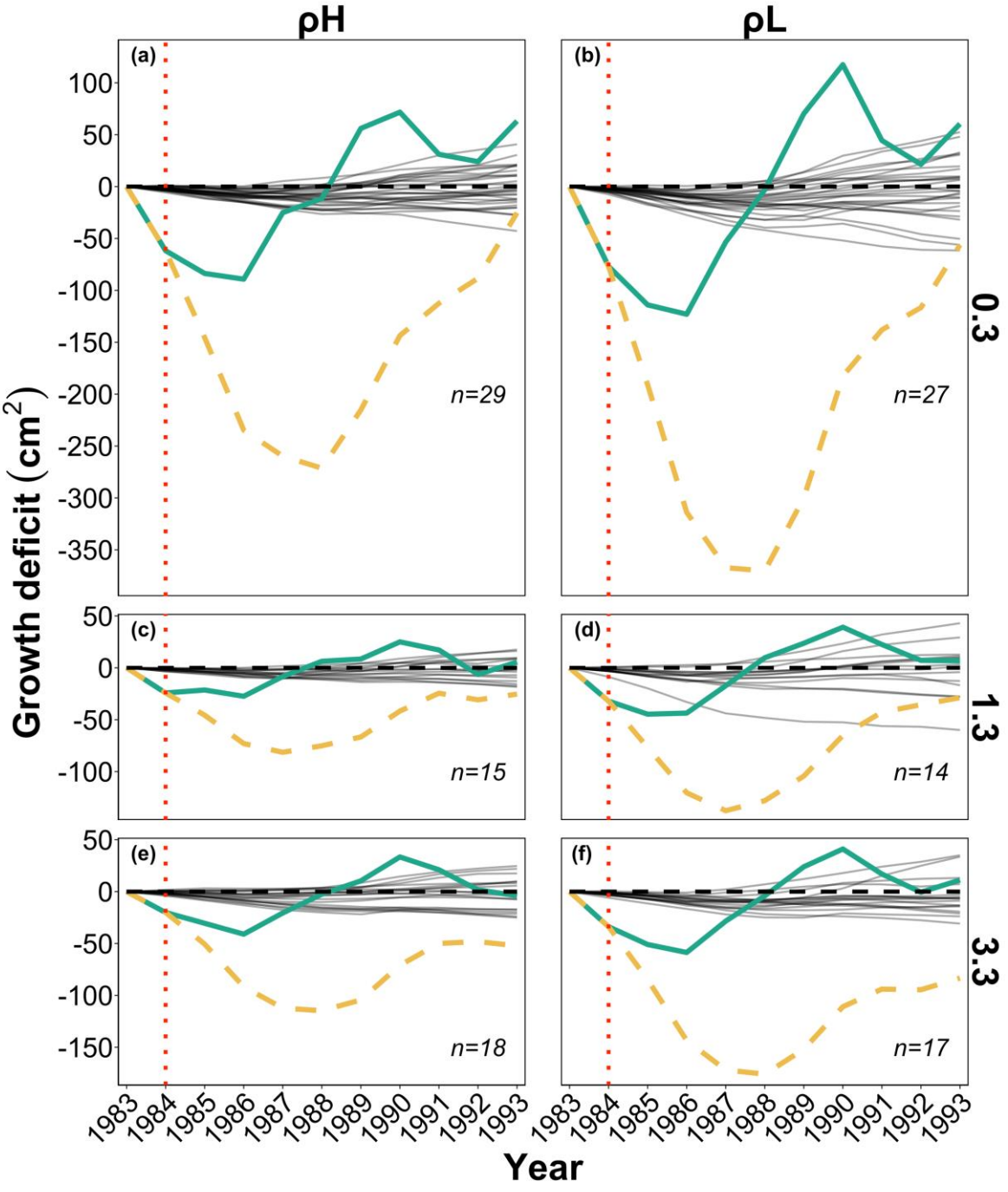

**Figure 4** – Growth deficit derived from the difference between observed and forecasted growth (BAI). Chronology level annual growth deficit summed over time, representing individual tree cumulative growth deficit at a given stem height (grey lines), stand *annual* deficit calculated by summing annual growth deficit for all chronologies at a given stem height in a given year (solid green line) and the *cumulative* stand growth deficit calculated annually by summing the annual stand deficit over time (dashed yellow line) in the high density ($\rho_H$) and low density ($\rho_L$) stands at 0.3m (a, b), 1.3m (c, d) and 3.3m (e, f) stem heights. Annual values were calculated for the drought year in 1984 (vertical dotted red line) and the subsequent 9 years (1985-1993) while *n*= the sample size for each stem height in the respective density treatment.

# 4. Discussion

Using dynamic regression models to forecast both tree growth rates and sizes in a scenario where extreme drought was absent enabled us to estimate patterns of forest response to drought. Our approach ensured annual climate is explicitly accounted for in both the pre-drought and forecasted periods, capturing each chronology's historical relationship between climate and growth prior to the drought event, as well as the autocorrelated nature inherent in radial tree growth from year to year. In doing so, we identified that post-drought annual growth rates can recover or even exceed those that might have been expected if no drought had occurred. This pattern of compensatory growth in a post-recovery phase resulted in the reclamation of some of the lost BA at all stem heights in both high and low density stands. Equally, we showed how patterns in growth resilience at the

stand level are the product of the temporal stratification of drought recovery at the level of individual trees, meaning assessments based purely on the average or stand level response (Huang et al., 2018) miss important variation and non-linearities in growth and size recovery dynamics. These non-linearities are only detectable when the temporal scale and resolution of assessment is over longer (up to nine years in this study) and finer (annually) timescales than commonly practiced (Bose et al., 2020; Gazol et al., 2017). By demonstrating how the importance of some stand attributes (e.g. stand density and pre-drought growth rates ans sizes) on growth recovery dynamics varies depending on the point during the recovery period, we provide evidence that assessing forest resilience annually over an extended post-drought period can provide a more comprehensive understanding of forest response to drought whilst highlighting limitations in approaches that use pre- and post-drought growth averages.

### 4.1. The temporal frame of resilience assessment

The linear increase in resilience (*Rs*) with the size of the integration period used to calculate average growth can be explained by observing the pattern of growth recovery. In this study, two years post-drought (1986) is the point of lowest absolute annual growth, after which a period of progressive growth recovery begins. As resilience (*Rs*) is often calculated as the ratio of pre-drought and post-drought growth averages (Gazol et al., 2018), continually increasing the size of this post-drought integration period will inevitably be reflected by a corresponding increase in resilience. As we demonstrate, the choice of integration period risks systematically biasing the calculation of resilience since increasingly large integration periods result in increasingly high values of resilience at all stem heights, influencing both our interpretation and understanding drought response. Similarly, this property makes the

584 comparability of resilience values difficult across study systems where the same integration
585 period has not been used to calculate pre- and post-drought growth averages e.g. Merlin et
586 al., (2015) and Serra-Maluquer et al., (2018). This change in resilience with the choice of
587 pre- and post-drought period is in keeping with other recent work that highlights the
588 limitations of considering only a single post-drought integration window (Schwarz et al.,
589 2020). Instead, we advocate assessing resilience at an annual resolution (Anderegg et al.,
590 2015; Huang et al., 2018; Kannenberg et al., 2019a; Martínez-Vilalta et al., 2012) to retain
591 important information regarding the temporal dynamics of forest drought response.
592
593 While mixed-model results indicate that *Gr* changes over time at all stem heights (**Table 2**),
594 contrary to our hypothesis, there was no differences in *Gr* between stem heights at any
595 point during drought recovery (**Fig. 2** and **Fig. S8 (d)**). However, mechanisms allowing the
596 targeted allocation of carbon below ground or above ground could indicate a decoupling of
597 tree-ring signals from gross primary productivity (Kannenberg et al., 2019b), which in turn
598 should lead us to question how representative resilience indices based solely on radial
599 growth are of whole tree resilience.
600
601 The observed non-linearities in *Gr* and drought legacy may be linked to post-drought
602 alterations in carbon allocation strategy. Such alterations could occur at the expense of
603 radial growth via the upregulation of photosynthesis (Kannenberg et al., 2019b), the
604 reparation and expansion of the canopy (Kannenberg et al., 2019b) or roots and fungal
605 hyphae (Børja et al., 2017). Such shifts in carbon allocation under drought have been
606 documented in *P. sylvestris* (Fernández-De-Uña et al., 2017) and could lead to the continued
607 decline in radial growth immediately after drought observed in this study. Subsequent radial

608 growth recovery may only then begin once the repair and expansion of roots and
609 mycorrhizal networks and repair of foliage have been made, shifting allocation patterns
610 back to compensate for losses in radial growth. Similarly, drought induced damage to xylem
611 and hydraulic architecture (Adams et al., 2017) may conceivably lead to reductions in radial
612 growth at the expense of metabolically costly repair. While the ecophysiological processes
613 that drive these observed patterns were not the focus of this study, mechanisms that allow
614 the preferential allocation of carbon (Hagedorn et al., 2016) could indicate a more plastic
615 and adaptive plant response to drought than current indices based on radial growth imply
616 and question current estimates of drought induced losses in biomass.
617

618 **4.2. Overgrowth, size recovery and post-recovery dynamics**

619 Stand-level growth recovery occurred around 4-5 years after drought, varying slightly with
620 stem height and density treatment (**Fig. 4**). However, individual trees were highly variable in
621 the time taken to recover (**Fig. 3**). Stand level recovery time is slightly longer than global
622 averages of 1-4 years (Anderegg et al., 2015) but two years longer than reported in a similar
623 study of *P. sylvestris* (Martínez-Vilalta et al., 2012). We continued to track annual growth
624 performance relative to forecast growth rates up to nine years post-drought and identified a
625 widespread pattern of 'overgrowth' i.e. growth that occurred in excess of that forecasted.
626 While the year in which annual stand growth turned from a deficit to a surplus (indicating
627 complete growth recovery) was relatively synchronous across stem heights and stand
628 densities, the magnitude of stand overgrowth differed. This pattern of radial overgrowth for
629 some trees in a post-recovery phase meant that all stem heights in both density treatments
630 recovered a considerable portion of the BA lost in the years immediately following drought
631 (relative to the forecasted no-drought scenario).

Patterns in *Gr* and overgrowth at the stand level were clearly the result of the disproportionate influence of individual trees in both density treatments at all stem heights, supporting our second hypothesis. The staggered return of individuals to forecasted growth rates (**Fig. 3**) was reflected in the increasing stratification of individual tree performance over time (**Fig. 4**). While most trees recovered to forecasted growth rates, some trees appeared to benefit from drought (being larger than forecasted in a no-drought scenario), particularly in the latter stages of the observed nine-year period, while others remained smaller than forecasted (**Fig. 4**), the net effect of which resulted in the observed reclamation of some lost BA.

To our knowledge this is the first study to document such patterns of overgrowth and size recovery following extreme drought in mature trees by extending the temporal window and increasing the temporal resolution of assessment. While attempts to quantify the cumulative impact of drought on radial growth during the recovery period are uncommon (*c.f.* Thurm et al., 2016), we demonstrate the importance of considering post-recovery growth dynamics when measuring the totality of drought impact. As noted by Gessler et al., (2020), the existence of compensatory growth *i.e.* increased function post-drought relative to pre-drought, is widely acknowledged in other ecological systems but has received little attention in stress-ecological studies. Indeed, compensatory growth has been documented in fish (Álvarez, 2011; Won and Borski, 2013), moths (Kecko et al., 2017), grasses (Østrem et al., 2010) and recently in seedlings of *P. sylvestris* (Seidel et al., 2019). By constraining the period of resilience assessment to either a pre-defined post-drought period or to the point at which growth returns to a historic norm implicitly assumes this point is where drought

legacy ends. However, our findings show that this assumption is not necessarily justified, with the legacy of drought extending far beyond a return to reference growth levels and even becoming positive for some trees.

By failing to document patterns in the recovery of lost BA, management decisions to increase overall forest resilience such as targeted tree removal or the selection of species for climate adaptation may be made prematurely on incomplete information. To illustrate this point using data from the present study, an assessment of the studied trees at a stem height of 0.3m in the lower density stand ($\rho_L$) (*n = 27*) three years after drought would indicate a cumulative loss of BA of 367 $cm^2$ (**Table S1**). However, the same assessment after nine years would indicate a much smaller loss in BA of only 56 $cm^2$ relative to forecasted values (**Table S1**). Thus, the severity of drought impact and choice of management designed to increase forest resilience depends on the post-drought period being considered. With a global push towards forest expansion to help deal with the challenges of a changing climate yet an increasing awareness of the associated risks and trade-offs (Anderegg et al., 2020; Doelman et al., 2020), decisions that are informed by the interplay between forest structure, drought resilience and the temporal dynamics of forest recovery will become increasingly important to ensure the continuity of forests ecosystems.

We caution that the patterns of overgrowth documented here are from a single experimental site and dependant on the accuracy of forecasted growth values. As such, the existence of patterns of overgrowth elsewhere needs to be established before wider conclusions can be drawn as to the importance or pervasiveness of such a mechanism. However, where extreme droughts are occurring with increasing frequency, intensity or

duration, the presence of overgrowth in a post-recovery phase could itself become maladaptive by leaving trees more susceptible to future drought impacts, the concept of *structural overshoot* (Jump et al., 2017). As a result, we argue that understanding the longer-term temporal dynamics of both growth and size recovery are crucial but largely overlooked components in studies on forest resilience, with clear implications for estimates of both historic and future drought induced losses of above ground biomass.

### 4.3. Temporal dependency of structural drivers

By explicitly modelling the observed non-linearity in *Gr*, we were able to explore the temporal dynamics of drought impact and investigate whether stand attributes such as pre-drought size, growth rate or stand density were (dis)advantageous for *Gr* throughout recovery. Contrary to our third hypothesis, we found that there was no simple relationship between faster growing, larger or more densely spaced trees and *Gr*. When considered annually, the interaction between growth rates in the pre-drought year ($BAI_{1983}$) and time highlighted that trees growing faster prior to drought had significantly higher *Gr,* but only between 1985 and 1987 and not during the drought year itself (1984) or in the post-recovery phase. These results differ to those reported by Martínez-Vilalta et al., (2012) who noted faster pre-drought growth negatively impacted drought recovery in *P. sylvestris* for three years immediately following drought. However, in contrast to this present study, Martínez-Vilalta et al., (2012) did not include climate variables as predictors when estimating growth in this post-drought period, or consider post-drought timescales longer than three years.

Stand density and pre-drought tree size also showed clear temporal dependacies in their relationship with *Gr*, corresponding to particular phases of the post-drought period. Again, contrary to our expectations, the higher density stand showed significantly higher *Gr* than the lower density stand but only for two years, during the period of continued growth decline (1985 -1986). In contrast and as expected, larger trees did show consistently lower *Gr*, but only from 1986 onwards (once the continued growth decline reversed and recovery began) and not during the drought year itself. This latter result is in keeping with other work that found larger trees suffer more under drought (Bennett et al., 2015). The opposing positive and negative influence of pre-drought growth and stand density vs pre-drought size respectively, highlights the importance of not reducing stand structure down to a single metric (Forrester, 2019).

The positive or negative impact of pre-drought stand attributes on individual recovery trajectories may result in changes in the competitive or functional dominance of individual trees. The decoupling of size and growth means that some trees contribute disproportionately to stand growth relative to their size (West, 2018). As such, directional shifts in stand level growth rates will depend on how drought differentially impacts those trees that contribute more or less to stand growth. While not the focus of this study, persistent drought-induced shifts in functional dominance both within and between species have been documented previously (Cavin et al., 2013) and the persistance with which pre-drought growth impacted meausres of *Gr* documented here could indicate a shift or amplification in the competitive status of individuals. Our analysis highlights that not all trees contributed equally to stand level recovery. The divergence of recovery responses seems to show that those trees that recovered early became dominant in terms of growth

and stayed dominant, while those that failed to recover settled into a new, lower-than-average growth regime.

As lower drought resilience is emerging as a good indicator of future mortality risk (DeSoto et al., 2020), lower historic resilience may be adapted in the future as a management tool to selectively remove susceptible trees and improve overall forest resilience. However, our results demonstrate that the importance of stand attributes that might be used to inform targeted tree removal to increase forest resilience (such as pre-drought tree growth rates, tree sizes or target stand densities) is temporally dependant. For example, in this study higher density stands were only found to be more resilient than lower density stands for two years (1986-1993), indicating that stand density was only important for increasing *Gr* for a small period of the overall recovery landscape. Consequently, we caution that if resilience concepts are to be successfully deployed to guide forest management, the selection of an appropriate temporal scale and resolution of resilience assessment will be key.

# 5. Conclusion

Growing concern as to the vulnerability of forests globally means a comprehensive understanding of forest response to drought is becoming increasingly important. Here we show that the temporal scale and resolution of approaches to assessing resilience are critical if we are to understand drought impact on stand growth and recovery dynamics. The application of dynamic regression to ecological questions using dendrochronological data demonstrated here is a promising approach to achieving such an increased understanding.

Notably, we identified the capacity of both tree and stand growth rates to return to, or even exceed those forecasted in a scenario where no drought occurred, a pattern that resulted in the partial reclamation of lost basal area. This process of overgrowth appears to be the product of the disproportionate influence of individual trees on stand level recovery. Higher pre-drought growth rates and stand density but lower pre-drought tree size is of clear importance for explaining patterns in growth resilience in our study, however the importance of these structural variables is temporally dependent, indicating more nuanced patterns of drought recovery than previous studies have suggested.

Future work should aim to investigate the roles of mortality and shifts in the competitive dominance of individual trees and their neighbourhoods to further understand the drivers of these temporally dependant patterns in stand behaviour. Similarly, investigating the pervasiveness of overgrowth, compensatory growth and the structural overshoot phenomenon in a post-recovery phase will be an important step in quantifying drought impact, with implications for both forest management targeted at increasing resilience, carbon budgeting and our understanding of drought legacy (Kannenberg et al., 2020).

## 6. Acknowledgements

This work was funded by Forest Research, the Scottish Forestry Trust and the University of Stirling. We thank Danni Thompson for her support and advice during manuscript preparation and Brad Duthie and Luc Bussiere for discussion and advice on statistical analysis. We are grateful to Barry Gardiner and colleagues for providing data and Adam Ash

for his insight and logistical help. We also thank the anonymous reviewers for their contribution in improving this manuscript. The authors have no conflicts of interest to declare.

## 7. Author Contributions

T.O. led conceptual development, methodological approach, analysis and the writing of the manuscript, M.P. contributed to concept development, manuscript production and facilitated data availability. T.C. contributed to the methodological approach, analysis and the writing of the manuscript, M.M. contributed to the manuscript production and A.J. contributed to the conceptual development and manuscript production.

## 8. Data availability statement

All data are archived and held at Stirling Online Repository for Research Data (DataSTORRE) and can be accessed here: https://datastorre.stir.ac.uk/handle/11667/163

## 9. ORCID

Thomas S Ovenden https://orcid.org/0000-0002-6957-1333

Mike Perks https://orcid.org/0000-0001-5608-802X

Toni-Kim Clarke https://orcid.org/0000-0002-7745-6351

Alistair S Jump https://orcid.org/0000-0002-2167-6451

Maurizio Mencuccini https://orcid.org/0000-0003-0840-1477

# 10. References


Adams, H.D., Zeppel, M.J.B., Anderegg, W.R.L., Hartmann, H., Landhäusser, S.M., Tissue, D.T., Huxman, T.E., Hudson, P.J., Franz, T.E., Allen, C.D., Anderegg, L.D.L., Barron-Gafford, G.A., Beerling, D.J., Breshears, D.D., Brodribb, T.J., Bugmann, H., Cobb, R.C., Collins, A.D., Dickman, L.T., Duan, H., Ewers, B.E., Galiano, L., Galvez, D.A., Garcia-Forner, N., Gaylord, M.L., Germino, M.J., Gessler, A., Hacke, U.G., Hakamada, R., Hector, A., Jenkins, M.W., Kane, J.M., Kolb, T.E., Law, D.J., Lewis, J.D., Limousin, J.M., Love, D.M., Macalady, A.K., Martínez-Vilalta, J., Mencuccini, M., Mitchell, P.J., Muss, J.D., O'Brien, M.J., O'Grady, A.P., Pangle, R.E., Pinkard, E.A., Piper, F.I., Plaut, J.A., Pockman, W.T., Quirk, J., Reinhardt, K., Ripullone, F., Ryan, M.G., Sala, A., Sevanto, S., Sperry, J.S., Vargas, R., Vennetier, M., Way, D.A., Xu, C., Yepez, E.A., McDowell, N.G., 2017. A multi-species synthesis of physiological mechanisms in drought-induced tree mortality. Nat. Ecol. Evol. 1, 1285–1291. doi:10.1038/s41559-017-0248-x

Allen, C.D., Breshears, D.D., McDowell, N.G., 2015. On underestimation of global vulnerability to tree mortality and forest die-off from hotter drought in the Anthropocene. Ecosphere 6, 1–55. doi:10.1890/ES15-00203.1

Allen, C.D., Macalady, A.K., Chenchouni, H., Bachelet, D., McDowell, N., Vennetier, M., Kitzberger, T., Rigling, A., Breshears, D.D., Hogg, E.H. (Ted., Gonzalez, P., Fensham, R., Zhang, Z., Castro, J., Demidova, N., Lim, J.H., Allard, G., Running, S.W., Semerci, A., Cobb, N., 2010. A global overview of drought and heat-induced tree mortality reveals emerging climate change risks for forests. For. Ecol. Manage. 259, 660–684. doi:10.1016/j.foreco.2009.09.001

818 Álvarez, D., 2011. Behavioral responses to the environment | Effects of Compensatory
819 Growth on Fish Behavior. Encycl. Fish Physiol. 1, 752–757. doi:10.1016/B978-0-12-
820 374553-8.00164-7
821 Anderegg, W.R.L., Kane, J.M., Anderegg, L.D.L., 2013. Consequences of widespread tree
822 mortality triggered by drought and temperature stress. Nat. Clim. Chang. 3, 30–36.
823 doi:10.1038/nclimate1635
824 Anderegg, W.R.L., Schwalm, C., Biondi, F., Camarero, J.J., Koch, G., Litvak, M., Ogle, K., Shaw,
825 J.D., Shevliakova, E., Williams, A.P., Wolf, A., Ziaco, E., Pacala, S., 2015. Pervasive
826 drought legacies in forest ecosystems and their implications for carbon cycle models.
827 Science (80-. ). 349.
828 Anderegg, W.R.L., Trugman, A.T., Badgley, G., Anderson, C.M., Bartuska, A., Ciais, P.,
829 Cullenward, D., Field, C.B., Freeman, J., Goetz, S.J., Hicke, J.A., Huntzinger, D., Jackson,
830 R.B., Nickerson, J., Pacala, S., Randerson, J.T., 2020. Climate-driven risks to the climate
831 mitigation potential of forests. Science (80-. ). 368. doi:10.1126/science.aaz7005
832 Bates, D., Mächler, M., Bolker, B.M., Walker, S.C., 2015. Fitting linear mixed-effects models
833 using lme4. J. Stat. Softw. 67. doi:10.18637/jss.v067.i01
834 Bennett, A.C., Mcdowell, N.G., Allen, C.D., Anderson-Teixeira, K.J., 2015. Larger trees suffer
835 most during drought in forests worldwide. Nat. Plants 1, 1–5.
836 doi:10.1038/nplants.2015.139
837 Biondi, F., Queaan, F., 2008. A Theory-Driven Approach to Tree-Ring Standardization :
838 Defining the Biological Trend from Expected Basal Area Increment. Tree-Ring Res. 64,
839 81–96.
840 Børja, I., Godbold, D.L., Sv, J., Nagy, N.E., Gebauer, R., Urban, J., Vola, D., Lange, H., Krokene,
841 P., Petr, Č., Eldhuset, T.D., 2017. Norway Spruce Fine Roots and Fungal Hyphae Grow

842 Deeper in Forest Soils After Extended Drough, in: Soil Biological Communities and
843 Ecosystem Resilience. pp. 123–142. doi:10.1007/978-3-319-63336-7
844 Bose, A.K., Gessler, A., Bolte, A., Bottero, A., Buras, A., Cailleret, M., Camarero, J.J., Haeni,
845 M., Hereş, A.M., Hevia, A., Lévesque, M., Linares, J.C., Martinez-Vilalta, J., Matías, L.,
846 Menzel, A., Sánchez-Salguero, R., Saurer, M., Vennetier, M., Ziche, D., Rigling, A., 2020.
847 Growth and resilience responses of Scots pine to extreme droughts across Europe
848 depend on predrought growth conditions. Glob. Chang. Biol. 1–17.
849 doi:10.1111/gcb.15153
850 Bunn, A., Korpela, M., Biondi, F., Campelo, F., Mérian, P., Qeadan, F., Zang, C., 2019. dplR:
851 Dendrochronology Program Library in R. R package version 1.7.0.
852 Cavin, L., Mountford, E.P., Peterken, G.F., Jump, A.S., 2013. Extreme drought alters
853 competitive dominance within and between tree species in a mixed forest stand. Funct.
854 Ecol. 27, 1424–1435. doi:10.1111/1365-2435.12126
855 Chmura, D.J., Anderson, P.D., Howe, G.T., Harrington, C.A., Halofsky, J.E., Peterson, D.L.,
856 Shaw, D.C., Brad St.Clair, J., 2011. Forest responses to climate change in the
857 northwestern United States: Ecophysiological foundations for adaptive management.
858 For. Ecol. Manage. 261, 1121–1142. doi:10.1016/j.foreco.2010.12.040
859 Dai, A., 2013. Increasing drought under global warming in observations and models. Nat.
860 Clim. Chang. 3, 52–58. doi:10.1038/nclimate1633
861 DeSoto, L., Cailleret, M., Sterck, F., Jansen, S., Kramer, K., Robert, E.M.R., Aakala, T.,
862 Amoroso, M.M., Bigler, C., Camarero, J.J., Čufar, K., Gea-Izquierdo, G., Gillner, S.,
863 Haavik, L.J., Hereş, A.M., Kane, J.M., Kharuk, V.I., Kitzberger, T., Klein, T., Levanič, T.,
864 Linares, J.C., Mäkinen, H., Oberhuber, W., Papadopoulos, A., Rohner, B., Sangüesa-
865 Barreda, G., Stojanovic, D.B., Suárez, M.L., Villalba, R., Martínez-Vilalta, J., 2020. Low

866 growth resilience to drought is related to future mortality risk in trees. Nat. Commun.
867 11, 1–9. doi:10.1038/s41467-020-14300-5
868 Doelman, J.C., Stehfest, E., van Vuuren, D.P., Tabeau, A., Hof, A.F., Braakhekke, M.C.,
869 Gernaat, D.E.H.J., van den Berg, M., van Zeist, W.J., Daioglou, V., van Meijl, H., Lucas,
870 P.L., 2020. Afforestation for climate change mitigation: Potentials, risks and trade-offs.
871 Glob. Chang. Biol. 26, 1576–1591. doi:10.1111/gcb.14887
872 Drever, C.R., Peterson, G., Messier, C., Bergeron, Y., Flannigan, M., 2006. Can forest
873 management based on natural disturbances maintain ecological resilience? Can. J. For.
874 Res. 36, 2285–2299. doi:10.1139/x06-132
875 Fernández-De-Uña, L., Rossi, S., Aranda, I., Fonti, P., González-González, B.D., Cañellas, I.,
876 Gea-Izquierdo, G., 2017. Xylem and leaf functional adjustments to drought in pinus
877 sylvestris and quercus pyrenaica at their elevational boundary. Front. Plant Sci. 8, 1–12.
878 doi:10.3389/fpls.2017.01200
879 Forrester, D.I., 2019. Linking forest growth with stand structure: Tree size inequality, tree
880 growth or resource partitioning and the asymmetry of competition. For. Ecol. Manage.
881 447, 139–157. doi:10.1016/j.foreco.2019.05.053
882 Gazol, A., Camarero, J.J., Anderegg, W.R.L., Vicente-Serrano, S.M., 2017. Impacts of
883 droughts on the growth resilience of Northern Hemisphere forests. Glob. Ecol.
884 Biogeogr. 26, 166–176. doi:10.1111/geb.12526
885 Gazol, A., Camarero, J.J., Vicente-Serrano, S.M., Sánchez-Salguero, R., Gutiérrez, E., de Luis,
886 M., Sangüesa-Barreda, G., Novak, K., Rozas, V., Tíscar, P.A., Linares, J.C., Martín-
887 Hernández, N., Martínez del Castillo, E., Ribas, M., García-González, I., Silla, F., Camisón,
888 A., Génova, M., Olano, J.M., Longares, L.A., Hevia, A., Tomás-Burguera, M., Galván, J.D.,
889 2018. Forest resilience to drought varies across biomes. Glob. Chang. Biol. 24, 2143–

2158. doi:10.1111/gcb.14082

Gessler, A., Bottero, A., Marshall, J., Arend, M., 2020. The way back: recovery of trees from drought and its implication for acclimation. New Phytol. doi:10.1111/nph.16703

Grace, J., Norton, D.A., 1990. Climate and Growth of Pinus Sylvestris at Its Upper Altitudinal Limit in Scotland: Evidence from Tree Growth-Rings. J. Ecol. 78, 601. doi:10.2307/2260887

Hagedorn, F., Joseph, J., Peter, M., Luster, J., Pritsch, K., Geppert, U., Kerner, R., Molinier, V., Egli, S., Schaub, M., Liu, J.F., Li, M., Sever, K., Weiler, M., Siegwolf, R.T.W., Gessler, A., Arend, M., 2016. Recovery of trees from drought depends on belowground sink control. Nat. Plants 2, 1–5. doi:10.1038/NPLANTS.2016.111

Halekoh, U., Højsgaard, S., 2014. A kenward-Roger approximation and parametric bootstrap methods for tests in linear mixed models-the R package pbkrtest. J. Stat. Softw. 59, 1–32. doi:10.18637/jss.v059.i09

Hoffmann, N., Schall, P., Ammer, C., Leder, B., Vor, T., 2018. Drought sensitivity and stem growth variation of nine alien and native tree species on a productive forest site in Germany. Agric. For. Meteorol. 256–257, 431–444. doi:10.1016/j.agrformet.2018.03.008

Huang, M., Wang, X., Keenan, T.F., Piao, S., 2018. Drought timing influences the legacy of tree growth recovery. Glob. Chang. Biol. 24, 3546–3559. doi:10.1111/gcb.14294

Hyndman, R.J., Athanasopoulos, G., 2018. Forecasting: principles and practice. OTexts.

Hyndman, R.J., Athanasopoulos, G., Bergmeir, C., Caceres, G., Chhay, L., O'Hara-Wild, M., Petropoulos, F., Razbash, S., Wang, E., Yasmeen, F., 2020. forecast: Forecasting functions for time series and linear models. R package version 8.12.

Jump, A.S., Ruiz-Benito, P., Greenwood, S., Allen, C.D., Kitzberger, T., Fensham, R., Martínez-

914 Vilalta, J., Lloret, F., 2017. Structural overshoot of tree growth with climate variability
915 and the global spectrum of drought-induced forest dieback. Glob. Chang. Biol. 23,
916 3742–3757. doi:10.1111/gcb.13636
917 Jyske, T., Mäkinen, H., Kalliokoski, T., Nöjd, P., 2014. Intra-annual tracheid production of
918 Norway spruce and Scots pine across a latitudinal gradient in Finland. Agric. For.
919 Meteorol. 194, 241–254. doi:10.1016/j.agrformet.2014.04.015
920 Kannenberg, S.A., Maxwell, J.T., Pederson, N., D'Orangeville, L., Ficklin, D.L., Phillips, R.P.,
921 2019a. Drought legacies are dependent on water table depth, wood anatomy and
922 drought timing across the eastern US. Ecol. Lett. 22, 119–127. doi:10.1111/ele.13173
923 Kannenberg, S.A., Novick, K.A., Alexander, M.R., Maxwell, J.T., Moore, D.J.P., Phillips, R.P.,
924 Anderegg, W.R.L., 2019b. Linking drought legacy effects across scales: From leaves to
925 tree rings to ecosystems. Glob. Chang. Biol. 2978–2992. doi:10.1111/gcb.14710
926 Kannenberg, S.A., Schwalm, C.R., Anderegg, W.R.L., 2020. Ghosts of the past: how drought
927 legacy effects shape forest functioning and carbon cycling. Ecol. Lett. 23, 891–901.
928 doi:10.1111/ele.13485
929 Kecko, S., Mihailova, A., Kangassalo, K., Elferts, D., Krama, T., Krams, R., Luoto, S., Rantala,
930 M.J., Krams, I.A., 2017. Sex-specific compensatory growth in the larvae of the greater
931 wax moth Galleria mellonella. J. Evol. Biol. 30, 1910–1918. doi:10.1111/jeb.13150
932 Kerhoulas, L.P., Kolb, T.E., Hurteau, M.D., Koch, G.W., 2013. Managing climate change
933 adaptation in forests: A case study from the U.S. Southwest. J. Appl. Ecol. 50, 1311–
934 1320. doi:10.1111/1365-2664.12139
935 Kuznetsova, A., Brockhoff, P.B., Christensen, R.H.B., 2017. lmerTest Package: Tests in Linear
936 Mixed Effects Models . J. Stat. Softw. 82. doi:10.18637/jss.v082.i13
937 Lenth, R. V., 2016. Least-squares means: The R package lsmeans. J. Stat. Softw. 69.

938 doi:10.18637/jss.v069.i01
939 Lloret, F., Keeling, E.G., Sala, A., 2011. Components of tree resilience: Effects of successive
940 low-growth episodes in old ponderosa pine forests. Oikos 120, 1909–1920.
941 doi:10.1111/j.1600-0706.2011.19372.x
942 Lutz, J.A., van Wagtendonk, J.W., Franklin, J.F., 2010. Climatic water deficit, tree species
943 ranges, and climate change in Yosemite National Park. J. Biogeogr. 37, 936–950.
944 doi:10.1111/j.1365-2699.2009.02268.x
945 Manrique-Alba, À., Beguería, S., Molina, A.J., González-Sanchis, M., Tomàs-Burguera, M., del
946 Campo, A.D., Colangelo, M., Camarero, J.J., 2020. Long-term thinning effects on tree
947 growth, drought response and water use efficiency at two Aleppo pine plantations in
948 Spain. Sci. Total Environ. 728. doi:10.1016/j.scitotenv.2020.138536
949 Martínez-Vilalta, J., Lloret, F., 2016. Drought-induced vegetation shifts in terrestrial
950 ecosystems: the key role of regeneration dynamics. Glob. Planet. Change 144, 94–108.
951 doi:10.1016/j.gloplacha.2016.07.009
952 Martínez-Vilalta, J., López, B.C., Loepfe, L., Lloret, F., 2012. Stand- and tree-level
953 determinants of the drought response of Scots pine radial growth. Oecologia 168, 877–
954 888. doi:10.1007/s00442-011-2132-8
955 McDowell, N.G., Allen, C.D., Anderson-teixeira, K., Aukema, B.H., Bond-lamberty, B., Chini,
956 L., Clark, J.S., Dietze, M., Grossiord, C., Hanbury-brown, A., Hurtt, G.C., Jackson, R.B.,
957 Johnson, D.J., Kueppers, L., Lichstein, J.W., Ogle, K., Poulter, B., Pugh, T.A.M., Seidl, R.,
958 Turner, M.G., Uriarte, M., Walker, A.P., Xu, C., 2020. Pervasive shifts in forest dynamics
959 in a changing world. Science (80-. ). doi:10.1126/science.aaz9463
960 Merlin, M., Perot, T., Perret, S., Korboulewsky, N., Vallet, P., 2015. Effects of stand
961 composition and tree size on resistance and resilience to drought in sessile oak and

962 Scots pine. For. Ecol. Manage. 339, 22–33. doi:10.1016/j.foreco.2014.11.032
963 Misi, D., Puchałka, R., Pearson, C., Robertson, I., Koprowski, M., 2019. Differences in the
964 climate-growth relationship of Scots Pine: A case study from Poland and Hungary.
965 Forests 10, 1–12. doi:10.3390/f10030243
966 Nikinmaa, L., Lindner, M., Cantarello, E., Jump, A.S., Seidl, R., Winkel, G., Muys, B., 2020.
967 Reviewing the Use of Resilience Concepts in Forest Sciences. Curr. For. Reports 6, 61–
968 80.
969 Nowosad, J., 2019. pollen: Analysis of Aerobiological Data. R package version 0.71.
970 Office, M., Hollis, D., McCarthy, M., Kendon, M., Legg, T., Simpson, I., 2019. HadUK-Grid
971 Gridded Climate Observations on a 1km grid over the UK, v1.0.0.0 (1862-2017). Centre
972 for Environmental Data Analysis. doi:10.5285/2a62652a4fe6412693123dd6328f6dc8
973 Østrem, L., Rapacz, M., Jørgensen, M., Höglind, M., 2010. Impact of frost and plant age on
974 compensatory growth in timothy and perennial ryegrass during winter. Grass Forage
975 Sci. 65, 15–22. doi:10.1111/j.1365-2494.2009.00715.x
976 Pinheiro, J., Bates, D., DebRoy, S., Sarkar, D., 2020. R Core Team (2020) nlme: Linear and
977 Nonlinear Mixed Effects Models. R package version 3.1-148.
978 Redmond, M.D., 2019. CWD and AET function V1.0.1 (Version V1.0.0).
979 doi:http://doi.org/10.5281/zenodo.2530955
980 Robinson, E.L., Blyth, E., Clark, D.B., Comyn-Platt, E., Finch, J., Rudd, A.C., 2017. Climate
981 hydrology and ecology research support system meteorology dataset for Great Britain
982 (1961-2015) [CHESS-met] v1.2. NERC Environmental Information Data Centre.
983 Schwarz, J.A., Skiadaresis, G., Kohler, M., K., J., Schnabel, F., Vitali, V., Bauhus, J., 2020.
984 Quantifying growth responses of trees to drought - a critique of the Lloret-indicators
985 and recommendations for future studies. Curr. For. Reports.

986 doi:https://doi.org/10.32942/osf.io/5ke4f
987 Seidel, H., Matiu, M., Menzel, A., 2019. Compensatory growth of scots pine seedlings
988 mitigates impacts of multiple droughts within and across years. Front. Plant Sci. 10.
989 doi:10.3389/fpls.2019.00519
990 Seidl, R., Vigl, F., Rössler, G., Neumann, M., Rammer, W., 2017. Assessing the resilience of
991 Norway spruce forests through a model-based reanalysis of thinning trials. For. Ecol.
992 Manage. 388, 3–12.
993 Seo, J.W., Eckstein, D., Jalkanen, R., Rickebusch, S., Schmitt, U., 2008. Estimating the onset
994 of cambial activity in Scots pine in northern Finland by means of the heat-sum
995 approach. Tree Physiol. 28, 105–112. doi:10.1093/treephys/28.1.105
996 Serra-Maluquer, X., Mencuccini, M.M., Martínez-Vilalta, J., 2018. Changes in tree resistance,
997 recovery and resilience across three successive extreme droughts in the northeast
998 Iberian Peninsula. Oecologia 187, 343–354. doi:10.1007/s00442-018-4118-2
999 Sohn, J.A., Saha, S., Bauhus, J., 2016. Potential of forest thinning to mitigate drought stress:
1000 A meta-analysis. For. Ecol. Manage. 380, 261–273. doi:10.1016/j.foreco.2016.07.046
1001 Stovall, A.E.L., Shugart, H., Yang, X., 2019. Tree height explains mortality risk during an
1002 intense drought. Nat. Commun. 10, 1–6. doi:10.1038/s41467-019-12380-6
1003 Szejner, P., Belmecheri, S., Ehleringer, J.R., Monson, R.K., 2020. Recent increases in drought
1004 frequency cause observed multi-year drought legacies in the tree rings of semi-arid
1005 forests. Oecologia 192, 241–259. doi:10.1007/s00442-019-04550-6
1006 Thurm, E.A., Uhl, E., Pretzsch, H., 2016. Mixture reduces climate sensitivity of Douglas-fir
1007 stem growth. For. Ecol. Manage. 376, 205–220. doi:10.1016/j.foreco.2016.06.020
1008 van der Maaten-Theunissen, M., van der Maaten, E., Bouriaud, O., 2015. PointRes: An R
1009 package to analyze pointer years and components of resilience. Dendrochronologia 35,

34–38. doi:10.1016/j.dendro.2015.05.006

Vanhellemont, M., Sousa-Silva, R., Maes, S.L., Van den Bulcke, J., Hertzog, L., De Groote, S.R.E., Van Acker, J., Bonte, D., Martel, A., Lens, L., Verheyen, K., 2018. Distinct growth responses to drought for oak and beech in temperate mixed forests. Sci. Total Environ. 650, 3017–3026. doi:10.1016/J.SCITOTENV.2018.10.054

Vicente-Serrano, S.M., Beguería, S., López-Moreno, J.I., 2010. A multiscalar drought index sensitive to global warming: The standardized precipitation evapotranspiration index. J. Clim. 23, 1696–1718. doi:10.1175/2009JCLI2909.1

Vitali, V., Büntgen, U., Bauhus, J., 2017. Silver fir and Douglas fir are more tolerant to extreme droughts than Norway spruce in south-western Germany. Glob. Chang. Biol. 23, 5108–5119. doi:10.1111/gcb.13774

Vitali, V., Forrester, D.I., Bauhus, J., 2018. Know Your Neighbours: Drought Response of Norway Spruce, Silver Fir and Douglas Fir in Mixed Forests Depends on Species Identity and Diversity of Tree Neighbourhoods. Ecosystems 21, 1215–1229. doi:10.1007/s10021-017-0214-0

West, P.W., 2018. Use of the Lorenz curve to measure size inequality and growth dominance in forest populations. Aust. For. 81, 231–238. doi:10.1080/00049158.2018.1514578

Won, E.T., Borski, R.J., 2013. Endocrine regulation of compensatory growth in fish. Front. Endocrinol. (Lausanne). 4, 1–13. doi:10.3389/fendo.2013.00074

Xu, C., McDowell, N.G., Fisher, R.A., Wei, L., Sevanto, S., Christoffersen, B.O., Weng, E., Middleton, R.S., 2019. Increasing impacts of extreme droughts on vegetation productivity under climate change. Nat. Clim. Chang. 9, 948–953. doi:10.1038/s41558-019-0630-6

Zang, C.S., Buras, A., Esquivel-Muelbert, A., Jump, A.S., Rigling, A., Rammig, A., 2019.

1034 Standardized drought indices in ecological research: Why one size does not fit all. Glob.
1035 Chang. Biol. 1–3. doi:10.1111/gcb.14809
1036
1037